Numerical Simulations of the Effects of Droplet Size and Concentration on Vapour-Droplet JP-10/Air Detonations

Lijuan Liu, Qi Zhang[*]

State Key Laboratory of Explosion Science and Technology, Beijing Institute of Technology, 100081 Beijing, China
[*]*E-mail: qzhang@bit.edu.cn*

Abstract: Two-dimensional simulations were conducted for JP-10 mono-dispersed vapour-droplet detonation in air, based on the detonation mechanism for clouds and validation of the extending critical droplet size limits in previous tests. In the simulations, the discrete phase model combined with the droplet evaporation and droplet breakup models was used. Utilizing a wide range of mono-dispersed droplet sizes and initial droplet concentrations, all cases of JP-10 droplets with a certain amount of pre-vaporized fuel can successfully achieve the deflagration to detonation transition. Detonation velocities at the equivalent concentration with droplet diameters no larger than 50 μm are in good agreement with the theoretical detonation velocities. The effects of droplet size and initial droplet concentration on the detonation behaviour were also investigated. Detonation velocities attained with droplet diameters below 50 μm appear to decrease very slightly with droplet size, but are almost equal to the velocity in gases. When the droplet diameter is above 50 μm, there is a decrease in simulated detonation velocity compared with fine droplets, and no secondary pressure peak was observed. For fuel-rich combustion, detonation velocities decrease rapidly with an increase in initial droplet concentration, and post-wave pressure fluctuation was obviously irregular, caused by the secondary local explosion of the droplets.

1   Introduction

The pulse detonation engine (PDE) is a promising new engine, which uses a detonation wave instead of a deflagration wave for the combustion process.

The deflagration to detonation transition (DDT) in PDEs is being numerically investigated by computational fluid dynamics (CFD) methodology for performance evaluation for different combustible fuel/air regimes. The jet fuel JP-10 has been widely used for aviation fuel and PDE purposes [1]. JP-10 is considered the most potent fuel due to its high calorific value and chemical availability; in addition, its low volatility is specifically designed to minimize flammability and explosion hazards. Until now, most of the existing literature on hydrocarbon detonations [2, 3] and hydrogen detonations [4, 5] has dealt with detonations of combustible fuels in the gaseous state. Little work has been performed on JP-10 being used in liquid fuel/oxidizer multiphase detonations, mainly because of the difficulty in obtaining reliable detonations when considering the atomization requirements, mixing timescales and evaporation [6-8].

The droplet size has been found to be a crucial influence on the detonation parameters. The droplet shattering rate, which determines the chemical energy release rate behind the blast wave, depends to a large extent on the droplet size. Experimental studies have also reported that the detonation velocity in heterogeneous mixtures is a function of droplet size. Earlier, Dabora *et al*. [9] revealed that the multiphase detonation velocity is in general lower than an ideal Chapman-Jouguet (CJ) velocity. The smallest droplet size studied was 290 μm in diameter and the largest observed velocity deficit was ~30-35% for 2600 μm droplets. Bowen *et al*. [10] observed self-sustained detonations in decane fogs, of 2 μm mean diameter, at near CJ velocities. More recently, Burcat and Eidelman [11, 12] found that in the range 50-500 μm initial droplet radius, the detonation velocity was inversely proportional to the reaction zone width behind the shock front; specifically, the detonation velocity attained with 50 μm droplets was almost equal to that in gases.

Brophy *et al*. [13] revealed that to obtain successful detonation for a JP-10/air aerosol, a Sauter mean diameter (SMD) below 3 μm and a large fraction of fuel vapour must be present. The numerical dependence of detonation performance on droplet diameter and evaporation rate reported by Cheatham and Kailasanath [14-16] agrees well with experimental results [13]. Tangirala and Dean [17] performed numerical analyses for stoichiometric two-phase JP-10/air detonations with droplet diameters of 3-10 μm, and achieved satisfactory performances of the single ideal PDE. They also concluded that smaller droplet sizes and some pre-vaporization of the fuel substantially expedites DDT. More recently, experimental results indicated that an SMD below 10 μm can be achieved with a JP-8 fuel pressure greater than 8 MPa, and only 6 MPa is necessary for achieving the characteristics favourable for detonation of preheated fuel [18]. Since cell sizes of JP-10 are similar to JP-8, little attention was devoted to JP-10

detonation, and it was theorized that JP-10 ought to detonate in a similar manner if JP-8 detonated in a PDE. In addition, droplet breakup of dispersed carbon-in-water suspensions when exposed to radiation was previously investigated [19].

In the work reported here, an idealized confined geometry, energy source, evaporation rate and sufficient evaporation time were used to obtain a certain amount of vaporized fuel. Utilizing a wide range of droplet sizes and initial droplet concentrations, and taking into account the effects of the droplet breakup model, two-dimensional simulations and analysis of multiphase detonations in JP-10/air mixtures were performed. Additionally, droplet combustion behaviour with respect to the effects of droplet size and initial droplet concentration were numerically investigated.

2   Numerical Models

2.1 Governing equations of gas phase and discrete phase

The continuous phase model solves the compressible Navier-Stokes equations using the SIMPLE algorithm, and the standard k-ε turbulent model. The governing equations are the compressible Euler equations with a chemical reaction gas system in a two-dimensional Cartesian coordinate system, with the dependent variable vector Q, convective flux vectors E and F, and source vector H:

$$\frac{\partial Q}{\partial t} + \frac{\partial E}{\partial t} + \frac{\partial F}{\partial t} = H \tag{1}$$

The discrete phase model (DPM) and stochastic tracking model were used to predict the trajectory of a discrete phase particle by integrating the force balance on the particle. This force balance equates the particle inertia with the forces acting on the particle (for the x direction), and can be written as:

$$\frac{du_p}{dt} = F_D\left(u - u_p\right) + \frac{g_x(\rho_p - \rho)}{p_p} + F_x \tag{2}$$

where u is the fluid phase velocity; u_p is the particle velocity (m/s); $F_D\ (u-u_p)$ is the drag force per unit particle mass (N); ρ_p is the density of the particle (kg/m³); ρ is the fluid density; F_x is an additional acceleration, force/unit particle mass (N).

2.2 Droplet evaporation and breakup model

Droplet particles evaporate by being heated up by the surrounding gas. The vaporization from a discrete phase droplet is initiated when the temperature of the droplet T_p (K) reaches the vaporization temperature T_{vap}, and continues until the droplet reaches the boiling point, T_{bp}, or until the droplet's volatile fraction is completely consumed.

The evaporation rate is governed by gradient diffusion, with the flux of vapour into the gas phase related to the gradient of the vapour concentration between the droplet surface and bulk gas:

$$N_i = k_c(C_{i,s} - C_{i,\infty}) \tag{3}$$

where N_i is the molar flux of vapour (kmol/m²·s), k_c is the mass transfer coefficient (m/s), $C_{i,s}$ and $C_{i,\infty}$ are the vapour concentrations at the droplet surface and in the bulk gas (kmol/m³), respectively.

The wave breakup model that is appropriate for high-Weber-number flows was used for calculating droplet breakup. In this model, breakup of droplet parcels is calculated by assuming that the radius of the newly formed droplets, r, is proportional to the wavelength of the fastest-growing unstable surface wave on the parent droplet, Λ:

$$r = B_0 + \Lambda \tag{4}$$

where B_0 is a breakup time constant set equal to 0.61. The rate of change of droplet radius in the parent parcel is given by

$$\frac{da}{dt} = -\frac{(a-r)}{\tau}, r \leq a \tag{5}$$

where the breakup time, τ, is given by

$$\tau = \frac{3.726\,B_1\,a}{\Lambda\Omega} \tag{6}$$

Values of B_1 can range between 1 and 60, depending on the injector characterization.

2.3 Parameter settings

The configuration modelling of the cylindrical tube was 0.06 m in diameter and 1 m in length with the two ends closed. The geometry appears to be more than sufficient for that presently required for a successful detonation based on studies

on DDT of fuel/air mixtures [20]. Due to the symmetrical geometry, only half of the flow field was chosen for the computing area. The mesh spacing is $\Delta x = 1$ mm and $\Delta y = 1$ mm inside the tube, with mesh generations and monitoring points of the flow field shown in Figure 1. The geometry was the same as in our previous parallel report [21] and experimental and numerical studies; hence, a verification of the same numerical method is not explained again here.
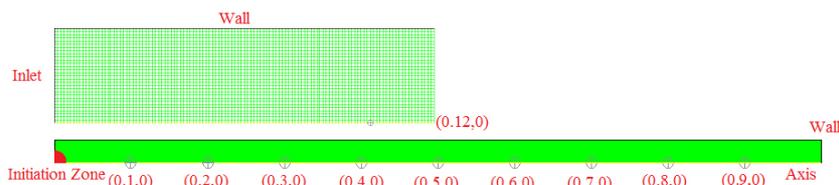
Figure 1. Mesh generations and monitoring points of the flow field (units/m)

As the boundary conditions, all tube walls were set as typical no-slip, no-leakage and adiabatic. In the absence of gravity, it was assumed that the mono-dispersed JP-10 droplets before the ignition delay time were homogeneously mixed with the air in the tube. As in related experimental conditions, DPM is used here in simulations of detonation in specific multiphase JP-10/air mixtures. The ignition scheme is direct detonation rather than involving a pre-detonator or a driver tube, and without obstacles or a Shchelkin spiral. As the initial and boundary conditions, the ignition region with high temperature and pressure is a semicircle of radius 1.5 cm at the left end, with high initial pressure $p = 30p_0$ and temperature $T = 10T_0$, respectively, and in the remaining region $p = p_0$, $T = T_0$, where p_0 and T_0 are the standard pressure and temperature. The specific parameters are listed in Table 1.

**Table 1.** Simulated detonation parameters of JP-10 liquid

Parameter	Value
Activation energy [J·kmol^{-1}]	1.26e+8 [22]
Pre-exponential factor [kmol·m^{-3}·s^{-1}]	7.84e+11[22]
Standard state enthalpy [J·kmol^{-1}]	−2e+8 [23]
Standard state entropy [J·kmol^{-1}·K^{-1}]	345222.4 [24]
Density [kg·m^{-3}]	940 [25]
Specific heat ratio [J·kg^{-1}·K^{-1}]	Piece-wise, linear in temperature [24, 26]
Enthalpy of vaporization [J·kg^{-1}]	376000 [27]
Boiling point [K]	460 [28]
Saturated vapour pressure [Pa]	Piece-wise, linear in temperature [26, 29]

3   Results and Discussion

In the present work, a velocity surface injector was used to generate small unheated droplets during the injection process and to control the initial droplet fuel concentrations. The initial droplet concentration range was 70 g/m³, 90 g/m³ (equivalence ratio of 1), 150 g/m³, 200 g/m³, 300 g/m³ to 500 g/m³ and the droplet diameter range was 3 μm, 5 μm, 10 μm, 20 μm, 50 μm, 80 μm and 100 μm.

3.1 Validation of the droplet models

Figure 2 depicts the molar fraction of pre-vaporized JP-10 versus the initial droplet concentration. With the same ignition delay time and droplet size, the JP-10 vapour molar fraction increases with initial droplet concentration but gradually stabilizes, mainly because the droplet evaporation process is affected by variations in thermodynamic and test parameters, such as droplet evaporation rate constants, ignition delay time, droplet size, initial droplet concentration, *etc*. A relatively larger droplet, for example, takes a longer time to evaporate. There is no necessity for all of the liquid phase to be converted to the vapour phase, but a sufficient amount of vapour fuel must be present for the detonation process to proceed.
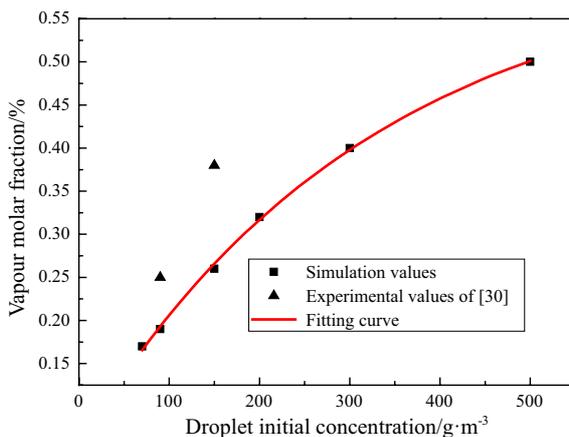

Figure 2.   JP-10 vapour molar fraction versus initial droplet concentration in fuel/air mixtures

The total amount of pre-vaporized fuel depends on the temperature-dependent saturated vapour pressure of the fuel; and thus, the total vapour molar fraction will be stabilized even when the initial droplet concentration continues to increase, which is reasonably consistent with the experimental results of Zhang

and Liu [30]. Thus, simulations using the droplet evaporation and breakup models presented here have been validated by experimental work.

After the injection of fuel into the tube, JP-10 droplets were initially and partially vaporized to achieve a favourable amount of vapour during the ignition delay process, as is shown in Figure 3. This is to facilitate the subsequent detonation process of the multiphase JP-10/air mixture.
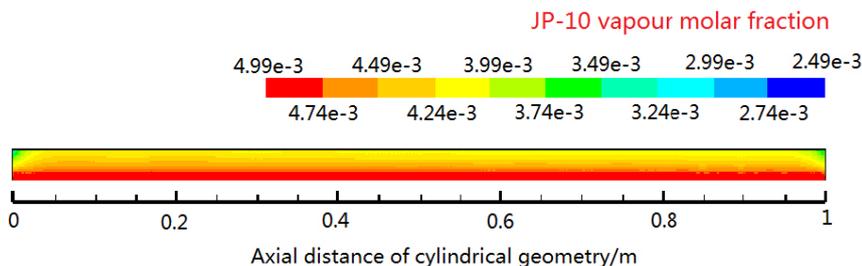

Figure 3. Molar fraction of JP-10 vapour in a multiphase fuel/air mixture before ignition

3.2 Droplet size effect on detonation velocity

For the clouds composed of gaseous oxidizer and liquid fuel with diameters below 50 µm, the detonation process is mainly subject to the ultimate vaporization speed of the fuel droplets in the detonation wave front. In the presence of the detonation wave front, a strong discontinuity of temperature and pressure in the cloud exists; at that time, the fuel droplets in the cloud are vaporized at the ultimate speed and mixed with the surrounding gaseous oxidizer, and then release energy to achieve detonation and sustain the continued propagation of the leading shock wave. Since the evaporation process is within 10^{-6} s due to the small droplet size, cloud detonation can be quite similar to that of a homogeneous gas; therefore, for cloud detonation of fuel droplets on the scale of microns, simulated detonation velocities agree well with the ideal CJ velocity in gases [16].

The JP-10 droplet concentration (c_{JP-10}^{d}, in g/m^3) and the average JP-10 vapour molar fraction (c_{JP-10}^{v}) in the fuel/air mixture before ignition are provided attached to Figure 4. In order to study the effect of droplet size on the detonation velocity in vapour-droplet JP-10/air mixtures, simulations were conducted with different ignition delay times, aiming to achieve similar JP-10 vapour molar fractions, despite the greatly varied evaporation rate with different droplet sizes. It should be pointed out that the average c_{JP-10}^{v} was obtained by estimation considering the non-uniform vapour-droplet distribution; however, small variations in the vapour concentration have little effect on the detonation performance in specified

vapour-droplet multiphase mixtures, mainly because the main parameters that affect the detonation velocity are the droplet evaporation and breakup rates, which is further explained below.
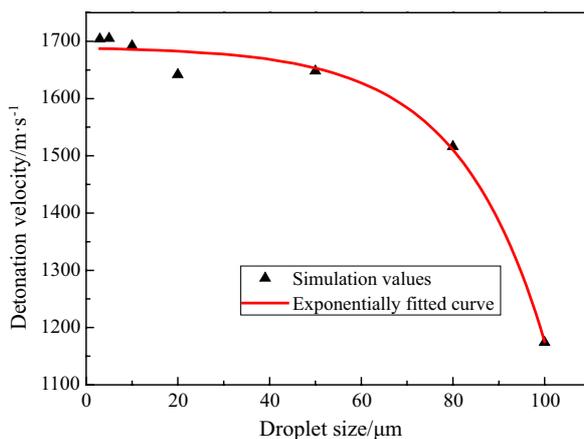
Figure 4.   Effect of JP-10 droplet size on detonation velocity at the equivalent concentration of 90 g/m^3 – the simulated values were: (1) 3 μm: $_{JP-10}^d$= 62 g/m^3, *avg.* c_{JP-10}^v= 0.50%; (2) 5 μm: $_{JP-10}^d$= 65 g/m^3, *avg.* c_{JP-10}^v= 0.41%; (3) 10 μm: $_{JP-10}^d$= 73 g/m^3, *avg.* c_{JP-10}^v= 0.30%; (4) 20 μm: $_{JP-10}^d$= 71 g/m^3, *avg.* c_{JP-10}^v = 0.33%; (5) 50 μm: $_{JP-10}^d$= 70 g/m^3, *avg.* c_{JP-10}^v= 0.31%; (6) 80 μm: $_{JP-10}^d$= 68 g/m^3, *avg.* c_{JP-10}^v= 0.34%; (7) 100 μm: $_{JP-10}^d$= 74 g/m^3, *avg.* c_{JP-10}^v= 0.28%

As seen from Figure 4, the droplet size has a significant effect on the detonation velocity, and fuel droplets in the region of 100 μm can also develop self-sustaining detonation. For this limited short tube, the detonation velocity decreased rapidly when the droplet size was greater than 50 μm, and large deficits from gaseous CJ detonation velocities were observed only for larger sized droplets. Here we preliminarily obtained an exponentially fitted curve to provide a prediction model, and the correlation between detonation velocity and droplet diameter was: *D = 1690.31-2.69133×exp(0.05254×d)*.

Due to the complex phenomena in the detonation reaction zone, this process cannot be explained by a simple droplet exfoliation mechanism, and a new mechanism was proposed, attributed to droplet deformation-breakup − local explosion in a cloud detonation. Specifically, after the leading shock wave, a large difference in velocity between the airflow and droplets can accelerate droplet motion and cause lateral droplet deformation so that the small particles rapidly generated at the rear of the droplets, vaporize and then cause acute explosion.

The energy released in the form of a second shock wave and local explosions sustains the leading shock wave and continuously causes the deformation, exfoliation and breakup of the droplets.
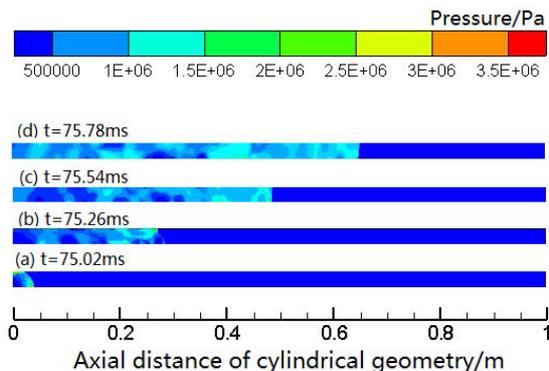
3.3 Droplet size effect on detonation pressure

Figure 5 shows the pressure profiles of JP-10 vapour and droplets of 5 μm and 100 μm diameter, and Figure 6 shows the pressure distributions of JP-10 vapour and droplets of 100 μm diameter. It may be seen that the detonation irregularity for 100 μm droplets was caused by the secondary local explosion. For the detonation pressure curve from 5 μm droplets, no secondary peak of fine particles was observed after the sharp drop of the detonation wave front, while for 100 μm droplets, post-wave pressure fluctuations were obviously irregular.

According to the aforementioned cloud detonation mechanism, for the two-phase detonation with droplet diameters below 50 μm, the time consumed in droplet breakup, within 10^{-6} s, is close to the delay time in gaseous detonation. Detonation velocities from less than 50 μm droplets agree well with the theoretical detonation velocities, and detonation behaviour in multiphase fuel/air mixtures are similar with those of gas detonations. However, when the droplet size is larger than 50 μm, the time required for droplet deformation and breakup increases with droplet size. The energy loss outside the reaction zone increases in the meantime, which leads to an increase in reaction zone width and a large deficit of the simulated detonation velocity with respect to theoretical values.
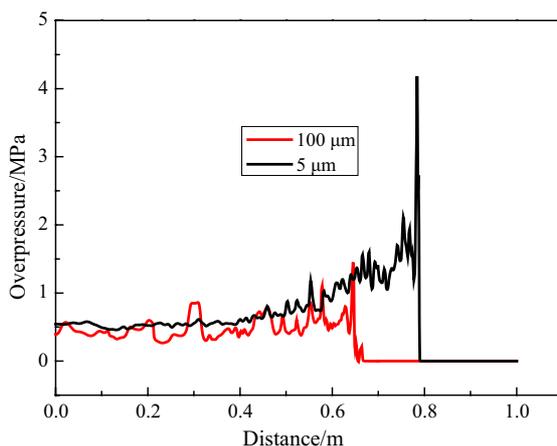
**Figure 5.**   Pressure profiles after ignition of JP-10 vapour and JP-10 droplets of 5 μm and 100 μm

Figure 6. Pressure distributions after ignition of JP-10 vapour and JP-10 droplets of 100 μm

3.4 Droplet concentration effect on detonation velocity

The simulation results of various initial JP-10 concentrations with a homogeneous droplet diameter of 50 μm were compared with previous experimental and numerical results [31-33]. As indicated in Figure 7, the detonation velocity reaches the maximum value at a stoichiometric JP-10/air (90 g/m^3) mixture. For fuel-lean combustion, the detonation velocity decreases slightly with an increase in initial droplet concentration; while for fuel-rich combustion, the detonation velocity decreases abruptly with initial droplet concentration, however, a tight coupling of the combustion and shock waves, expected for a CJ detonation, indicates flame acceleration and reliable detonation.

Since little attention was devoted to a broader range of initial droplet concentrations, we are not able at present to compare some results for larger droplet concentrations with CJ values. As with the aforementioned studies on the droplet size effect, in order to investigate the initial droplet concentration effect, $_{JP-10}$^{d} and average c_{JP-10}^{v} are also shown below Figure 7, and similar values of JP-10 vapour molar fractions for all cases were also obtained. As is shown in Figure 7, most of the velocities reach up to above 1600 m/s, and the velocity in the stoichiometric JP-10/air mixture is almost equal to, but still slightly lower than, the CJ velocity presented by Schauer *et al*. [31].
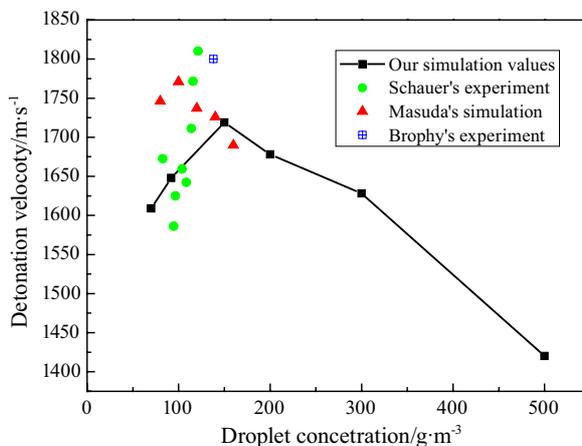
Figure 7. Effect of initial droplet concentration on detonation velocity with an homogeneous droplet size of 50 μm – the simulated values were: (1) 70 g/m^3: $_{JP-10}^d$= 55 g/m^3, *avg.* c_{JP-10}^v = 0.28%; (2) 90 g/m^3: $_{JP-10}^d$= 64 g/m^3, *avg.* c_{JP-10}^v = 0.31%; (3) 150 g/m^3: $_{JP-10}^d$= 133 g/m^3, *avg.* c_{JP-10}^v = 0.29%; (4) 200 g/m^3: $_{JP-10}^d$= 180 g/m^3, *avg.* c_{JP-10}^v = 0.31%; (5) 300 g/m^3: $_{JP-10}^d$= 245 g/m^3, *avg.* c_{JP-10}^v = 0.30%; (6) 500 g/m^3: $_{JP-10}^d$= 463 g/m^3, *avg.* c_{JP-10}^v = 0.38%

3.5 Droplet concentration effect on detonation pressure

Figure 8 shows the overpressure history profiles for homogeneous droplets of 50 μm diameter and different initial droplet concentrations at different locations in the tube. The pressures at a low concentration are relatively stable at different monitoring locations, and the pressures at a lean concentration of 70 g/m^3 and at the stoichiometric concentration 90 g/m^3 are basically similar at 3 MPa. However, the pressure gradually becomes unstable when the initial droplet concentration is increased; for example, an obvious pressure fluctuation occurs at the concentration of 200 g/m^3. When the initial concentration reaches up to 300 g/m^3, the pressures fluctuate significantly, mainly because a large amount of JP-10 vapour was instantaneously generated at higher concentrations, but was not involved in the detonation reaction.

(a) 70 g/m^3

(b) 90 g/m^3

(c) 200 g/m^3

(d) 300 g/m^3
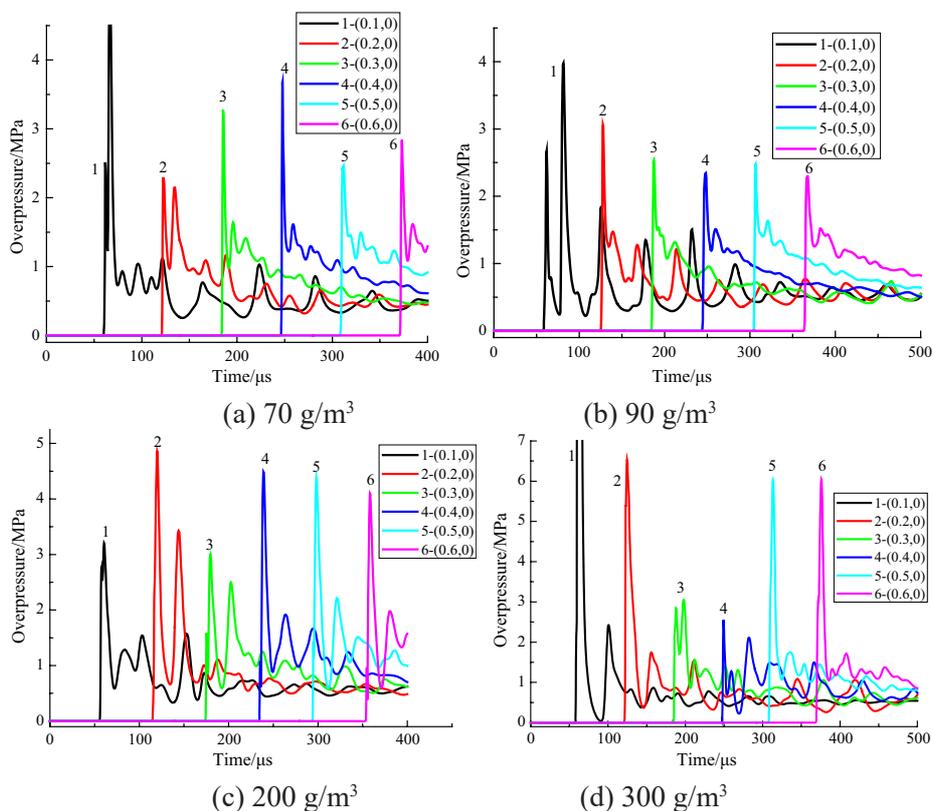
Figure 8.   Overpressure history profiles at different initial concentrations at different locations

As the pressure wave propagated through different monitoring points along the downstream tube, a sudden jump to a high pressure spike was observed due to overdriven detonation [18]. After the wave front passes, pressure relaxation occurs to a near steady plateau pressure at each point. It should be noted that the pressure profiles are much noisier than those of the gaseous state, also shown in our previous simulation report [21]. This is because a discontinuity of energy release occurs with all of the fuel in the liquid phase. A rise in pressure at the pressure wave front, a steady plateau pressure behind the detonation front, as well as a tight coupling of combustion and the pressure wave front are indicative of a successful detonation.

Our simulated detonation pressures are reasonably consistent with the detonation pressure of JP-10 droplets obtained from Brophy *et al.* [13] and Sandhu *et al.* [34]. The simulated detonation properties of JP-10 were also validated

suggesting further research scope in the development of relevant experiments on PDEs and cloud detonations.

4   Conclusions

The numerical model of vapour-droplet multiphase detonation presented here was validated to simulate JP-10 vapour-droplet multiphase detonation in air using DPM, combined with droplet evaporation and breakup models. The effects of droplet size and initial droplet concentration on the detonation properties were investigated. Simulations on mono-dispersed droplets of various diameters and initial concentrations indicated the necessity of small-sized droplets and near-equivalent initial concentrations to achieve the CJ velocity and pressure. The detonation transition was significantly enhanced and the critical droplet size limits for a limited short tube were extended.

In all of the cases studied here, mono-dispersed JP-10 droplets of various diameters with some pre-vaporized fuel successfully achieved a deflagration to detonation transition in air. The detonation velocities for droplets no larger than 50 μm appeared to decrease very slightly with the initial droplet size and but remained almost equal to those in gases. The detonation velocity decreased rapidly when the droplet size was greater than 50 μm, and there is a large deficit in the simulated detonation velocity in comparison with theoretical values. For the detonation pressure curve of very fine droplets, the normal secondary peak in the detonation of fine particles was not obvious, while for 100-μm-diameter droplets, fluctuation of the post wave pressure was obviously irregular and caused by the secondary local explosion of fuel droplets.

In terms of the effect of the initial concentration, for a fuel-rich combustion, the detonation velocity decreased rapidly with an increase in the initial droplet concentration, and pressure fluctuations were obviously observed. The detonation velocity of a stoichiometric JP-10/air mixture with 50 μm droplets reached a near-CJ velocity, and simulated detonation pressures were reasonably consistent with the available literature. The investigated detonation properties of JP-10 obtained should have significance for future research scope in the development of PDEs and cloud detonation for a broad audience.

References

[1] Wintenberger, E.; Shepherd, J. E. Model for the Performance of Airbreathing Pulse-Detonation Engines. *J. Propul. Power* **2006**, *22*(3): 593-603.

[2] Knystautas, R.; Guirao, C.; Lee, J. H.; Sulmistras, A. Measurements of Cell Size in Hydrocarbon-Air Mixtures and Predictions of Critical Tube Diameter, Critical Initiation Energy, and Detonability Limits. In: *Dynamics of Shock Waves, Explosions, and Detonations*. (Soloukhin, R. I.; Oppenheim, A. K.; Manson, N.; Bowen, J. R., Eds.) **1984**, pp. 23-37.

[3] Beeson, H. D.; McClenagan, R. D.; Bishop, C. V.; Benz, F. J. Detonability of Hydrocarbon Fuels in Air. In: *Dynamics of Detonations and Explosions: Detonations*. (Leyer, J.-C.; Borisov, A. A.; Kuhl, A. L.; Sirignano, W. A., Eds.) **1991**, pp. 19-36; ISBN 978-0-930403-97-3.

[4] Debnath, P.; Pandey, K. M. Numerical Investigation of Detonation Combustion Wave in Pulse Detonation Combustor with Ejector. *J. Appl. Fluid Mech.* **2017**, *10*(2): 1-10.

[5] Debnath, P.; Pandey, K. M. Exergetic Efficiency Analysis of Hydrogen-Air Detonation in Pulse Detonation Combustor Using Computational Fluid Dynamics. *Int. J. Spray Combust. Dyn.* **2017**, *9*(1): 44-54.

[6] Benedick, W. B.; Tieszen, S. R.; Knysautas, R.; Lee, J. H. S. Detonation of Unconfined Large-Scale Fuel Spray-Air Clouds. In: *Dynamics of Detonations and Explosions: Detonations*. (Leyer, J.-C.; Borisov, A. A.; Kuhl, A. L.; Sirignano, W. A., Eds.) **1991**, pp. 297-310; ISBN: 978-0-930403-97-3.

[7] Li, S. C.; Varatharajan, B.; Williams, F. A. Chemistry of JP-10 Ignition. *AIAA J.* **2001**, *39*(12): 2351-2356.

[8] Hutchins, T. E.; Metghalchi, M. Energy and Exergy Analyses of the Pulse Detonation Engine. *J. Eng. Gas Turbines Power* **2003**, *125*(4): 1075-1080.

[9] Dabora, E. K.; Raglan, K. W.; Nicholls, J. A. Drop-Size Effects in Spray Detonations. *Symposium (Int.) on Combustion*, Elsevier, **1969**, *12*(1): 19-26.

[10] Bowen, J. R.; Ragland, K. W.; Steffes, F. J.; Loflin, T. G. Heterogeneous Detonation Supported by Fuel Fogs or Films. *Symposium (Int.) on Combustion* **1971**, *13*(1): 1131-1139.

[11] Burcat, A.; Eidelman, S. Evolution of a Detonation Wave in a Cloud of Fuel Droplets, II- Influence of Fuel Droplets. *AIAA J.* **1980**, *18*(10): 1233-1236.

[12] Eidelman, S.; Burcat, A. The Mechanism of a Detonation Wave Enhancement in a Two-Phase Combustible Medium. *Symposium (Int.) on Combustion* **1981**, *18*(1): 1661-1670.

[13] Brophy, C. M.; Netzer, D. W.; Sinibaldi, J.; Johnson, R. High-Speed Deflagration and Detonation: Fundamentals and Control. In: *International Colloquium on Control and Detonation Processes* (Roy, G. D.; Frolov, S. M.; Netzer, D. W.; Borisov, A. A., Eds.), Moscow, Russia **2000**, pp. 207-222; ISBN 5938150019.

[14] Cheatham, S.; Kailasanath, K. Numerical Simulations of Multiphase Detonation in a Shock Tube. *41ˢᵗ Aerospace Sciences Meeting and Exhibit, Aerospace Sciences*

Meetings, Reno, NV **2003**, 1315.

[15] Cheatham, S.; Kailasanath, K. Multiphase Detonations in Pulse Detonation Engines. *42nd AIAA Aerospace Sciences Meeting and Exhibit, Aerospace Sciences Meetings*, Reno, NV **2004**, 306.

[16] Cheatham, S.; Kailasanath, K. Single-Cycle Performance of Idealized Liquid-Fueled Pulse Detonation Engines. *AIAA J*. **2005**, *43*(6): 1276-1283.

[17] Tangirala, V. E.; Dean, A. J. Investigations of Two-Phase Detonations for Performance Estimations of a Pulse Detonation Engine. *45th AIAA Aerospace Sciences Meeting and Exhibit, Aerospace Sciences Meetings*, Reno, NV **2007**, 1173.

[18] Wen, C. S.; Chung, K. M.; Lu, F. K.; Lai, W. H. Assessment of Flash-Boiling for Pulse Detonation Engines. *Int. J. Heat Mass Transfer* **2012**, *55*(11): 2751-2760.

[19] Xu, J.; Qiao, L.; Gao, J.; Chen, J. Droplet Breakup of Micro- and Nano-Dispersed Carbon-in-Water Colloidal Suspensions Under Intense Radiation. *Int. J. Heat Mass Transfer* **2014**, *78*: 267-276.

[20] Smirnov, N. N. Combustion and Detonation in Multiphase Media Containing a Liquid Fuel. *Combust., Explos. Shock Waves* **1998**, *24*(3): 340-349.

[21] Liu, L.; Zhang, Q.; Shen, S.; Li, D.; Lian, Z.; Wang, Y. Evaluation of Detonation Characteristics of Aluminum/JP-10/Air Mixtures at Stoichiometric Concentrations. *Fuel* **2016**, *169*: 41-49.

[22] Roux, S.; Cazalens, M.; Poinsot, T. Outlet-Boundary-Condition Influence for Large Eddy Simulation of Combustion Instabilities in Gas Turbines. *J. Propul. Power* **2008**, *24*(3): 541-546.

[23] Yin, D.; Chen, T.; Cong, P.; Yuan, S. Numerical Simulation of Combustion on JP-10 and RP-3. (in Chinese) *Journal of Naval Aeronautical and Astronautical University* **2008**, *23*(3): 1673-1522.

[24] Hudzik, J. M.; Asatryan, R.; Bozzelli, J. W. Thermochemical Properties of *exo*-Tricyclo[5.2.1.0(^{2,6})] decane (JP-10 jet fuel) and Derived Tricyclodecyl Radicals. *J. Phys. Chem. A* **2010**, *114*(35): 9545-9553.

[25] Harvey, B. G.; Wright, M. E.; Quintana, R. L. High-Density Renewable Fuels Based on the Selective Dimerization of Pinenes. *Energy Fuels* **2009**, *24*(1): 267-273.

[26] *Handbook of Aviation Fuel Properties*. Coordinating Research Council, Inc, DTIC selected copy, Atlanta, GA **1983**, pp. 46-47.

[27] Chickos, J. S.; Hillesheim, D.; Nichols, G.; Zehe, M. J. The Enthalpies of Vaporization and Sublimation of *exo*-and *endo*-Tetrahydrodicyclopentadienes at T = 298.15 K. *J. Chem. Thermodyn.* **2002**, *34*(10): 1647-1658.

[28] Bruno, T. J.; Huber, M. L.; Laesecke, A.; Lemmon, E. W.; Perkins, R. A. *Thermochemical and Thermophysical Properties of JP-10*. Technical Report NISTIR No. 6640-325, **2005**.

[29] Shepherd, J. E.; Austin, J.; Chao, T.; Pintgen, F.; Wintenberger, E.; Jackson, S.; *et al*. Detonation Initiation, Propagation, and Structural Response. In: *Proc. 14th ONR Propulsion Meeting* (Roy, G. D.; Mashayek F., Eds.), Chicago, IL **2001**, pp. 148-153.

[30] Zhang, Q.; Liu, X. Explosion Parameters of Gaseous JP-10/Air Mixtures. *Cent.*

Eur. J. Energ. Mater. **2016**, *13*(1): 261-270.

[31] Schauer, F.; Miser, C.; Tucker, C.; Bradley, R.; Hoke, J. Detonation Initiation of Hydrocarbon-Air Mixtures in a Pulsed Detonation Engine. 4*3rd AIAA Aerospace Sciences Meeting and Exhibit, Aerospace Sciences Meetings*, Reno, NV **2005**, 1343.

[32] Masuda, N.; Tangirala, V.; Benkiewicz, K.; Hayashi, A. K.; Tsuboi, N. Numerical Simulation of JP-10/Air Two-Phase Detonation. *Int. J. Energ. Mater. Chem. Propul.* **2008**, *7*(5): 421-436.

[33] Roy, G. D.; Frolov, S. M.; Borisov, A. A.; Netzer, D. W. Pulse Detonation Propulsion: Challenges, Current Status, and Future Perspective. *Prog. Energy Combust. Sci.* **2004**, *30*(6): 545-672.

[34] Sandhu, M.; Goel, A.; Sharma, R. K.; Soni, S. K.; Singh, A. Performance Comparison of Liquid Fuel Based Pulse Detonation System Using Different Liquid Fuel-Air Mixtures. *National Propulsion Conference*, Madras, India **2013**, 1-8.